Iran J Pediatr. 2016 December; 26(6):e6135. doi: 10.5812/ijp.6135.

Published online 2016 September 18. **Case Report**

Novel *FBLN5* Mutation of Congenital Autosomal Recessive Cutis Laxa With Isolated Right Ventricular Non-Compaction (RVNC): New Findings on Echocardiographic Speckle-Tracking Strain Imaging of RVNC

Elaheh Malakan Rad,[1,2,*] Ali-Akbar Zeinaloo,[1,2] Ariana Kariminejad,[3] Uwe Kornak,[4] Bjorn Fischer-Zirnsak,[2] and Masoud Mohamadpour[1,2]

[1]Department of Pediatrics, Tehran University of Medical Sciences, Tehran, IR Iran
[2]Children's Medical Center, Pediatrics Center of Excellence, Tehran, IR Iran
[3]Kariminejad-Najmabadi Pathology and Genetics Center, Tehran, IR Iran
[4]Institut fuer Medizinische Genetik und Humangenetik, Berlin-Brandenburg Centrum fuer Regenerative Therapien, Charite-Universitaetsmedizin Berlin, Berlin, Germany

[*]*Corresponding author*: Elaheh Malakan Rad, Department of Pediatrics, Tehran University of Medical Sciences, Tehran, IR Iran. E-mail: erad@tums.ac.ir

Received 2016 March 27; **Revised** 2016 August 21; **Accepted** 2016 September 07.

Abstract

We report on a novel mutation in a two-year-old child with autosomal recessive cutis laxa with severe generalized laxity of the skin, prematurely aged appearance, conjunctival chalasia, episodes of severe rectal prolapse, isolated right ventricular non-compaction, (RVNC), significant pulmonary hypertension at the systemic arterial pressure level, severe tricuspid regurgitation, corpulmonale secondary to recurrent pulmonary infections, and mixed pulmonary fibrosis and emphysema. Next generation sequencing of cutis laxa genes identified a novel homozygous mutation in the *FBLN5* gene (homozygous sequence alteration of c.907C > T [p. Gln303*] *FBLN5* [ENST00000342058]). Despite severe and generalized disorder in the patient's connective tissues, she had no primary valvar or vascular abnormalities in the heart. Complete speckle-tracking strain imaging (SI) by two-dimensional echocardiography showed decreased systolic longitudinal and transverse strain in the involved segment of the right ventricle (RV).

Keywords: Novel *FBLN5* Mutation, Autosomal Recessive Cutis Laxa, Right Ventricular Non-Compaction

1. Introduction

Cutis laxa (CL) is a rare dermatological disease secondary to disordered elastin formation. It may be congenital or acquired. Congenital CL may be autosomal recessive, autosomal dominant, or X-linked. Autosomal recessive CL (ARCL) is divided into five subtypes: type 1A, type 1B, type IIA, type IIB, and type III. Aortic aneurysm has been reported as a common finding in type 1A (1, 2). We report a new case of ARCL type 1A with a novel *FBLN5* mutation, right ventricular non-compaction, and no arterial or valvar involvement.

2. Case Presentation

A two-year-old child with a known diagnosis of ARCL type 1A was referred to the pediatric cardiology clinic with cyanosis, generalized edema, and mild respiratory distress. She was born to consanguineous parents (first-degree cousins). The first offspring of these parents was a healthy six-year-old boy. The second pregnancy was aborted due to unknown reasons at 24 weeks of gestation, and the third child of the family was our patient. The child had a history of multiple hospital admissions for pulmonary infections since early infancy. On physical examination, she was cyanotic with no clubbing. Her weight and height were below the 5th percentile for age, and her mental and motor development were normal. Her abdomen was protuberant secondary to a combination of ascites and abdominal distension. She had a prematurely aged face, down slanting palpebral fissures, periorbital edema, sagging cheeks, a long philtrum, a prominent nasolabial fold, severe wrinkling around the mouth, downturned corners of the mouth, wrinkling and skin folds in the trunk and limbs, hyperlaxity of joints, circumferential lines around the limbs, bilateral inguinal hernia, and abdominal hernia (Figure 1). A comparison of the clinical features of this patient with the previously reported cases with ARCL type 1A is shown in Box 1.

Cardiac auscultation revealed a loud P2 and a holosystolic regurgitant murmur of grade 3/6 in the tricuspid area. Electrocardiography revealed right-axis deviation and right ventricular hypertrophy, and a chest X-ray

Figure 1. Clinical Features of the Patient

A, shows the megalocornea at the neonatal period; B and C show the prematurely aged appearance of the child; C indicates the conjunctival chalasia due to chemosis; F and G show the wrinkled left leg and left hand of the patient.

showed right atrial and ventricular enlargement and consolidation in the right lung. Echocardiography also revealed significant enlargement of the right atrium and right ventricle, remarkable segmental right ventricular non-compaction near the right ventricular apex, and severe tricuspid regurgitation (TR), with a pressure gradient of 74 mmHg. Tricuspid annular systolic excursion (TAPSE) was decreased (12 mm). The inferior vena cava diameter was dilated and did not collapse with inspiration, indicative of an RA pressure of at least 20 mmHg (Figure 2). Hemoglobin and hematocrit were 18 gr/dL and 61.3%, respectively, suggesting chronic systemic oxygen desaturation.

Cardiac computed tomography angiography (CCTA) re-confirmed RVNC and excluded pulmonary thromboembolism. The patient's aorta was normal in diameter from the root to the bifurcation into iliac arteries. A high-resolution computed tomography scan (HRCT) of the chest demonstrated linear collapse consolidations, areas of emphysema, fibrosis, and pulmonary infection in the right lung. The patient's brain CT scan was normal.

After admission, treatment with digoxin, furosemide, spironolactone, and sildenafil was started, and non-invasive ventilation was applied. Shortly thereafter, the patient underwent intratracheal intubation and mechanical ventilation due to progressive worsening of her respiratory condition. After a few weeks, there was significant improvement of peripheral edema, ascites, and signs of right-sided heart failure; however, the patient continued to have a distended abdomen due to distension of the in-

Box 1. Comparison of Non-Cardiac and Cardiac Clinical Features of Homozygous Sequence Alteration of the c.907C > T (p. Gln303*) *FBLN5* (ENST00000342058) Mutation of Autosomal Recessive Cutis Laxa (our Case) With Previously Reported *FBLN5* Mutations of Cutis Laxa (Type 1A)

Comparison
Features not present in our case but present in other cases with autosomal recessive type 1a (gene defect in *Fbln5*)
Muscular hypotonia
Diaphragmatic defects
Scoliosis
Alopecia
Opacification of the cornea
Delay in motor development
Arterial tortuosity
Thick aortic valve
Prolapse of both mitral and tricuspid valves
Peripheral pulmonary artery stenosis
Supravalvular aortic stenosis
Beaked nose
Features not present in previous cases autosomal recessive type 1a (gene defect in *FBLN5*),but present in our case
Bilateral megalocornea appearance at birth with spontaneous normalization of the size of the cornea
Normal mitral and tricuspid valves
Right ventricular non-compaction
Normal bladder
Normal aorta and pulmonary artery
Pulmonary fibrosis
Features in common with previous cases
Conjunctival chalasia secondary to chemosis
Rectal prolapse
Bilateral inguinal hernia
Aged face with prominent nasolabial folds
Abdominal distension
Large ear lobes
Wrinkling of skin in the trunk and limbs
Progressive sagging of jowl since birth
Hyperlaxity of joints
Failure to thrive
Pulmonary emphysema and fibrosis
Cor pulmonale

testines that waxed and waned over time. After initial stabilization, we performed a comprehensive systolic and diastolic strain study by 2D speckle tracking echocardiography using the wall motion tracking (WMT) software of an Aplio 300 Toshiba cardiovascular echocardiography machine (Toshiba Medical Systems, Europe, B.V.) (3). We measured the RV systolic and diastolic strain and strain rate and displacement using the full right ventricular and left ventricular volume method (4).

End-diastole and end-systole were defined automatically by the software. Frame rate was set at $\geq$ 60 frame/second. The patient was in normal sinus rhythm

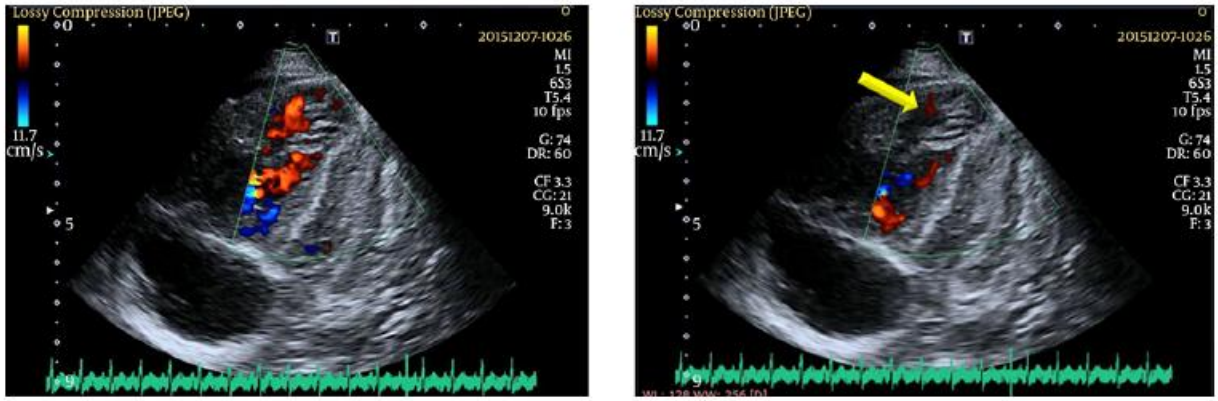

Figure 2. Prominent Non-Compaction Myocardium in the Apical-Septal Segment of the Right Ventricle, With the Blood Flow Entering the Spaces Between the Hyper-Trabeculations

during strain imaging. We obtained standard apical four-chamber, two-chamber, and long-axis views in three standard apical, middle, and basal levels. We stored three well-defined cardiac cycles for offline measurements. Each wall motion tracking (WMT) measurement was repeated three times, and the average values were considered. Using speckle-tracking 2D imaging, we measured the ejection fraction of all four chambers of the heart (Table 1). We also measured the ratio of total atrial ejection fraction to total ventricular ejection fraction, which was (29.44%)/(34.57%) (0.85%). We also investigated a new index of total atrial strain and total ventricular strain. We found:

- Abnormal post-systolic thickening in the transverse strain imaging of the segment with RVNC (Figure 3)

- Abnormal positive longitudinal strain in the opposing walls to the segment with RVNC (Figures 4 and 5).

- Abnormal biventricular total longitudinal systolic and diastolic strain, which may be indicative of RV-LV interaction (Figure 6).

- Decreased longitudinal and transverse strain in the segment with RVNC.

- Decreased right atrial ejection fraction relative to the left atrial ejection fraction (EF).

We also assumed that an examination of the outer layer of the septal wall of each ventricle can provide information about the interventricular septum. By comparison of longitudinal displacement of the septal outer layer of the RV and LV, we found that the difference in quantity of displacement between the base and the apex was higher in the RV than in the LV (7 mm versus 3 mm). Furthermore, the outer layer of the RV at the level of the segment with non-compaction had negative displacement at the end-systole (Figure 7).

Table 1. Measurement of Atrial and Ventricular Ejection Fraction Using Speckle-Tracking 2D Echocardiography

Chamber	Ejection Fraction(EF),%
Right atrium	15.08
Right ventricle	32.02
Left atrium	42.14
Left ventricle	54.84
Total atrial ejection fraction	29.46
Total ventricular ejection fraction	34.57

3. Discussion

ARCL type 1A is a very rare congenital connective tissue disorder (5). We report a new homozygous mutation of *FBLN5* (homozygous sequence alteration of c.907C > T [p. Gin303*] *FBLN5* [ENST00000342058]). This is also the first report of ARCL type 1A with isolated RVNC. We used two diagnostic criteria-hypertrabeculated to compact ratio > 3 and the maximal systolic thickness of the compacted septum < 8 mm for confirmation of diagnosis of RVNC (6, 7) On speckle tracking strain imaging of all four cardiac chambers in this case, we found reciprocal abnormal segmental findings in the walls opposed to the segment with RVNC. We suggest that the interventricular septum merits further study by speckle-tracking 2D-echocardiogaphic strain imaging. We accept that distinguishing the separate roles of RVNC and pulmonary hypertension in the aforementioned changes is only feasible if we repeat the examination after complete treatment of pulmonary hypertension.

Speckle-tracking 2D-echocardiography facilitates measurement of EF in all four chambers, regardless of the geo-

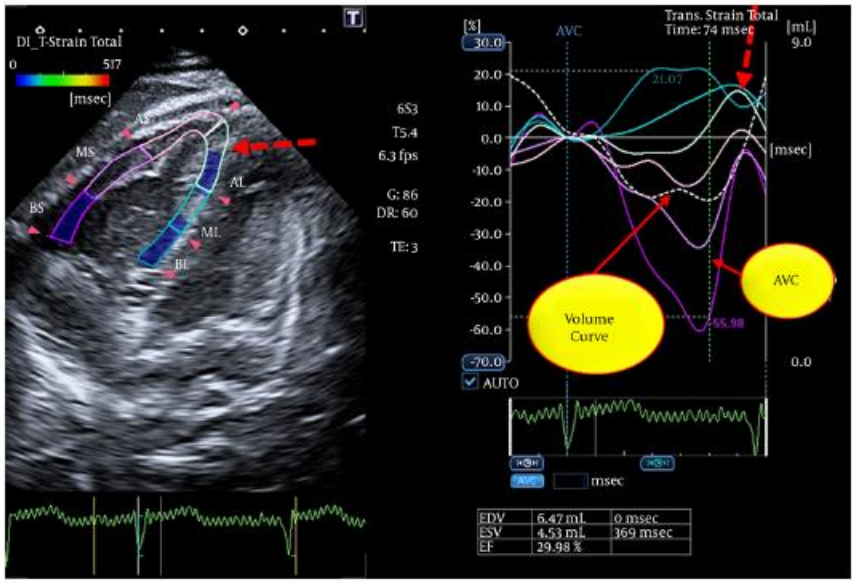

Figure 3. Abnormal Post-Systolic Thickening in the Transverse Strain Imaging of the Segment With RVNC

Figure 4. Abnormal Positive Longitudinal Strain in the Opposing Walls to the Segment With RVNC

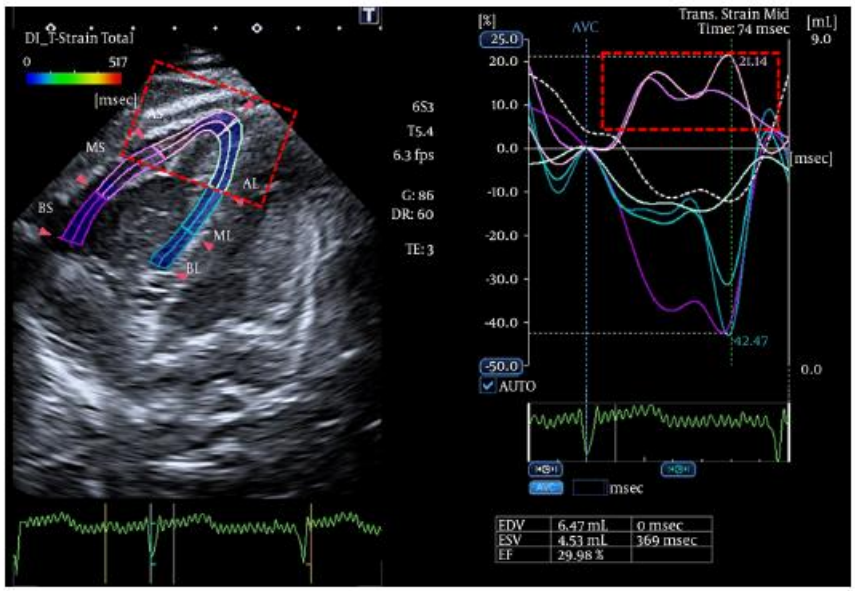

The curve in blue turquoise color shows the longitudinal strain (LS) in the non-compacted segment, and the light pink curve indicates the LS in the opposing wall.

metric assumptions needed in previous methods (8, 9). We propose the ratio of total atrial EF to total ventricular EF as an index of total cardiac function. However, this index must be validated, and normal values must be obtained.

Callewaert et al. and other investigators have reported pulmonary emphysema and vascular complications as two main characteristics of ARCL type I (10, 11). However, our case with the novel homozygous mutation has limited segments, with pulmonary emphysema and no vascular involvement. The dilated pulmonary artery in our case is due to long-standing severe pulmonary hypertension (PH) secondary to long-standing pulmonary disease. Severe tricus-

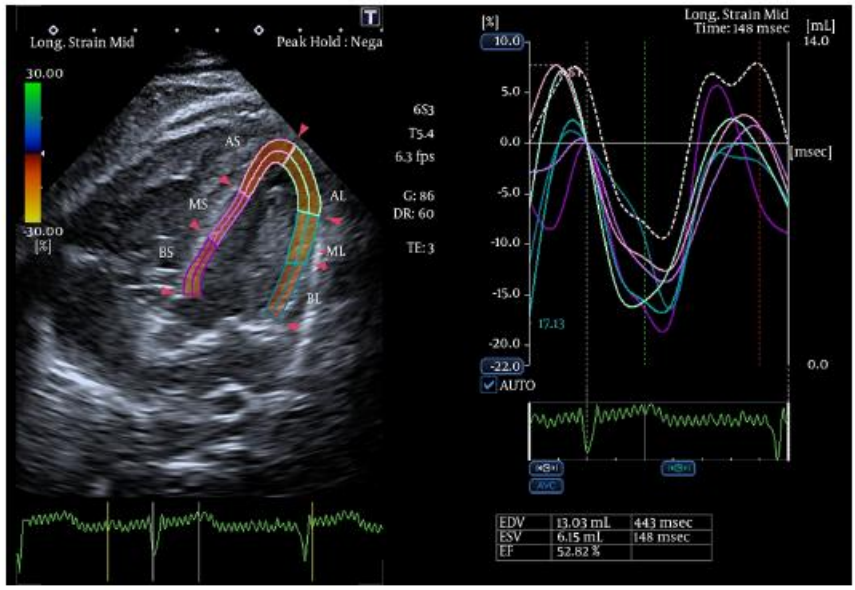

Figure 5. Longitudinal Strain of Opposing Walls of LV are Indicated for Comparison With the Opposing Walls of RV in Figure 4

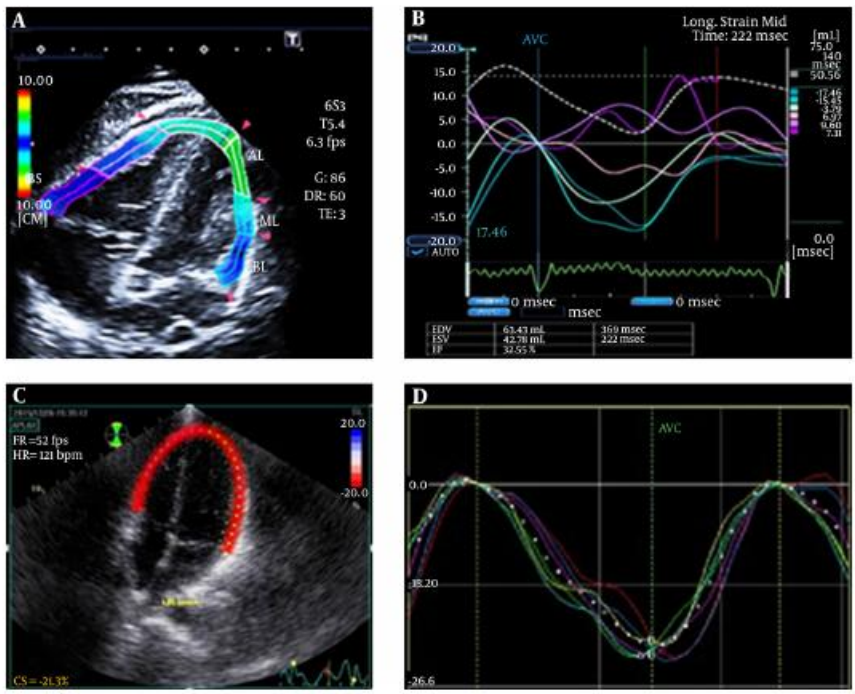

Figure 6. Comparison of biventricular strain in our patient with cutis laxa and RVNC with an age-matched normal child referred to the outpatient clinic for a benign murmur (N.B. the lower panel echocardiography was performed using a Vivid 7 echocardiography machine [GE Healthcare]).

pid regurgitation was due to annular dilation secondary to right-sided heart failure. After rigorous medical treatment, tricuspid regurgitation was completely improved.

Further investigation is necessary to explain the dilemma of diverse genotype-phenotype correlations in ARCL and the absence of primary involvement of cardiac

Figure 7. The Difference in Quantity of Displacement Between the Base and the Apex in RV and LV, Which is Higher in RV Than in LV (7 mm vs. 3 mm)

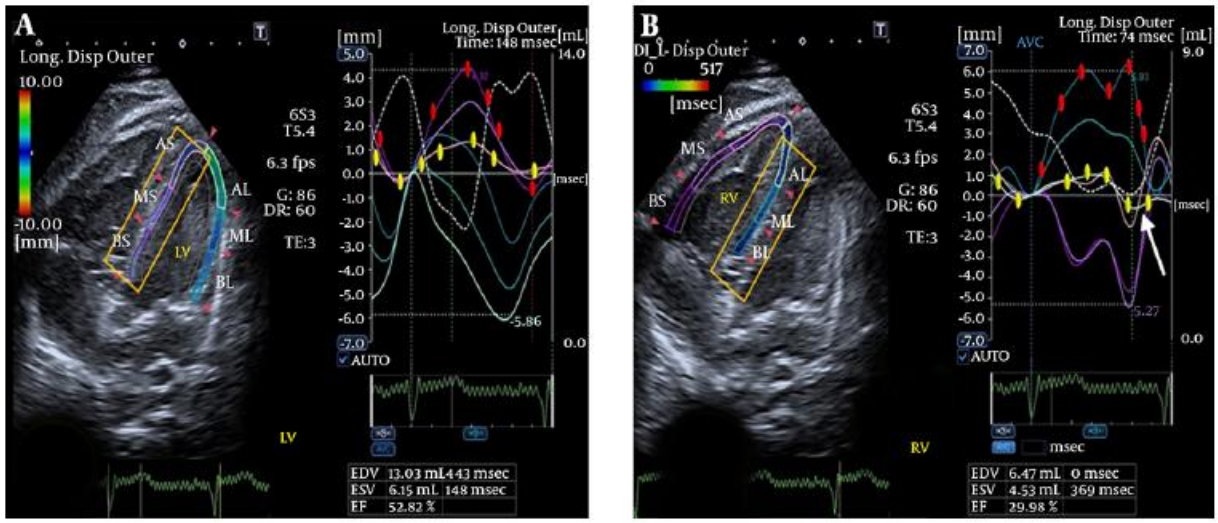

The outer layer of RV at the level of the segment with NC shows negative displacement at the end-systole (white arrow on B). B). (In each ventricle, the curves of longitudinal displacement of the opposing walls during systole and diastole are marked by yellow and red filled bullets on the curves).

valves and vessels despite severe, generalized elastinopathy.

Ventricular non-compaction is a genetic cardiomyopathy. Isolated RVNC in infants and children is extremely rare, with less than five cases reported to date (12). Neurologic evaluation is essential in patients with ventricular non-compaction (13). Neurologic examination of our patient was normal.

We addressed the reciprocal effects of RVNC on the opposing walls and on the LV in this study.

In summary, we introduced a novel mutation of ARCL type 1A with an isolated hereditary cardiomyopathy (RVNC) not previously reported.

Footnotes

Authors' Contribution: All the authors contributed to the final revision of the manuscript. Elaheh Malakan Rad drafted the initial version, carried out the echocardiographs, and performed the revisions. The co-authors and Ariana Kariminejad performed the genetic study.

Financial Disclosure: The authors have no financial disclosure to declare.

Funding/Support: The authors received no funding or support.

Statement of Parents' Consent: Parental consent was obtained for publication of this case and the illustrations of the patient.

References

1. Kumar P, Savant SS, Das A. Generalized acquired cutis laxa type 1: a case report and brief review of literature. *Dermatol Online J.* 2016;**22**(3) [PubMed: 27136630].
2. Berk DR, Bentley DD, Bayliss SJ, Lind A, Urban Z. Cutis laxa: a review. *J Am Acad Dermatol.* 2012;**66**(5):842. doi: 10.1016/j.jaad.2011.01.004. [PubMed: 22387031].
3. Lopez L, Colan SD, Frommelt PC, Ensing GJ, Kendall K, Younoszai AK, et al. Recommendations for quantification methods during the performance of a pediatric echocardiogram: a report from the Pediatric Measurements Writing Group of the American Society of Echocardiography Pediatric and Congenital Heart Disease Council. *J Am Soc Echocardiogr.* 2010;**23**(5):465–95. doi: 10.1016/j.echo.2010.03.019. [PubMed: 20451803] quiz 576-7.
4. Levy PT, Sanchez Mejia AA, Machefsky A, Fowler S, Holland MR, Singh GK. Normal ranges of right ventricular systolic and diastolic strain measures in children: a systematic review and meta-analysis. *J Am Soc Echocardiogr.* 2014;**27**(5):549–60. doi: 10.1016/j.echo.2014.01.015. [PubMed: 24582163].
5. Mohamed M, Voet M, Gardeitchik T, Morava E. Cutis Laxa. *Adv Exp Med Biol.* 2014;**802**:161–84. doi: 10.1007/978-94-007-7893-1_11. [PubMed: 24443027].
6. Elahi E, Kalhor R, Banihosseini SS, Torabi N, Pour-Jafari H, Houshmand M, et al. Homozygous missense mutation in fibulin-5 in an Iranian autosomal recessive cutis laxa pedigree and associated haplotype. *J Invest Dermatol.* 2006;**126**(7):1506–9. doi: 10.1038/sj.jid.5700247. [PubMed: 16691202].
7. Fazio G, Lunetta M, Grassedonio E, Gullotti A, Ferro G, Bacarella D, et al. Noncompaction of the right ventricle. *Pediatr Cardiol.* 2010;**31**(4):576–8. doi: 10.1007/s00246-010-9652-6. [PubMed: 20155258].
8. Gebhard C, Stahli BE, Greutmann M, Biaggi P, Jenni R, Tanner FC. Reduced left ventricular compacta thickness: a novel echocardiographic criterion for non-compaction cardiomyopathy. *J Am Soc Echocardiogr.* 2012;**25**(10):1050–7. doi: 10.1016/j.echo.2012.07.003. [PubMed: 22883316].

9. Cameli M, Mondillo S, Solari M, Righini FM, Andrei V, Contaldi C, et al. Echocardiographic assessment of left ventricular systolic function: from ejection fraction to torsion. *Heart Fail Rev.* 2016;**21**(1):77–94. doi: 10.1007/s10741-015-9521-8. [PubMed: 26712329].
10. Callewaert B, Su CT, Van Damme T, Vlummens P, Malfait F, Vanakker O, et al. Comprehensive clinical and molecular analysis of 12 families with type 1 recessive cutis laxa. *Hum Mutat.* 2013;**34**(1):111–21. doi: 10.1002/humu.22165. [PubMed: 22829427].
11. Kantaputra PN, Kaewgahya M, Wiwatwongwana A, Wiwatwongwana D, Sittiwangkul R, Iamaroon A, et al. Cutis laxa with pulmonary emphysema, conjunctivochalasis, nasolacrimal duct obstruction, abnormal hair, and a novel FBLN5 mutation. *Am J Med Genet A.* 2014;**164A**(9):2370–7. doi: 10.1002/ajmg.a.36630. [PubMed: 24962763].
12. Sert A, Aypar E, Aslan E, Odabas D. Isolated right ventricular noncompaction in a newborn. *Pediatr Cardiol.* 2013;**34**(8):1896–8. doi: 10.1007/s00246-012-0435-0. [PubMed: 22810045].
13. Stollberger C, Finsterer J. Septal hypertrabeculation/noncompaction: cardiac and neurologic implications. *Int J cardiol.* 2009;**132**(2):173–5.